

# Molecular Simulation of the Hydration of Ethene to Ethanol Using Ab Initio Potentials and Free Energy Curves

S. Tolosa Arroyo,\* J. C. Corchado Martin-Romo, A. Hidalgo Garcia, and J. A. Sansón Martín

Departamento de Química Física, Universidad de Extremadura, 06071 Badajoz, Spain

Received: July 23, 2007; In Final Form: September 19, 2007

Molecular dynamics simulations of aqueous solutions at infinite dilution of the reaction of water with ethene:  $\text{H}_2\text{O} + \text{CH}_2\text{CH}_2 \rightarrow \text{CH}_3\text{CH}_2\text{OH}$  were performed using Lennard-Jones 12-6-1 potentials to describe the solute–solvent interactions, and TIP3P to describe the water–water interactions. The Morokuma decomposition scheme of ab initio interaction energies at the SCF level and the dispersion component at the MP2 level were used to reproduce the molecular parameters of the solute–water interaction potentials. The results show that the functions that use the EX-PL-DIS-ES interaction model to describe the solvation of the reactant, transition state, and product systems lead to good values of the reaction ( $\Delta G$ ) and acceptable values of the activation ( $\Delta G^\ddagger$ ) free energy as compared with those from using AMBER-derived parameters, using the available theoretical and experimental data as referents.

## 1. Introduction

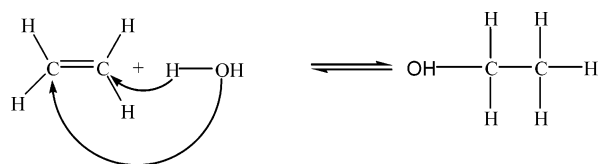
The study of chemical reactions in solution continues and is still one of the topics of most interest in quantum chemistry.<sup>1–15</sup> In view of the great number of interactions that take place, a quantum mechanical treatment of the whole system (considering the solute and all the solvent molecules) is computationally expensive, and recourse is made to approximate methods. Although there exist other procedures with an acceptable response to study the solvation of chemical systems (such as those which incorporate the effect of the solvent as a dielectric,<sup>16</sup> or those which employ a mixed quantum/molecular mechanics computational model, the QM/MM methods<sup>17</sup>), we shall use the classical method of molecular mechanics<sup>18</sup> using ab initio potentials to describe the solute–solvent interaction and the TIPnP potentials to describe the explicit solvent.

The description of the solute–solvent interaction will be based on the Lennard-Jones 12-6-1 analytical function whose molecular parameters are taken from fitting solute–solvent interaction energies calculated at the ab initio level,<sup>19–28</sup> instead of using the geometric-mean combining rules or parameter tables for model molecules. The solute charges are derived from a fit of the electrostatic component (ES) of the solute–water interaction energy, which will be denoted as ESIE in accordance with previous work. With respect to the molecular parameters of the van der Waals terms in the LJ(12-6) interaction potential, we employed a fitting procedure based on using different components of the interaction energy—in particular, the repulsion-exchange (EX), polarization (PL), and dispersion (DIS) components—to describe the repulsive and attractive contributions of the interaction.

The present work can be considered as a continuation of previous studies<sup>27</sup> in which the LJ(12-6-1) potential determined from the EX-PL-DIS-ES components was proposed to describe chemical reactions in aqueous solution. There are three main objectives pursued in this work: (a) to analyze, by means of the radial distribution functions and of the solute–solvent

interaction energies of the molecules that participate in the reaction, the molecular hydration, the exothermic character, and the energy barrier for this reactive process; (b) to confirm that our model potential and that the free energy curves obtained from solvent fluctuation are also applicable to chemical reactions in solution where one solvent molecule gets attached to the C=C double bond in a non-assisted concerted mechanism; and (c) to make some modifications to the procedure previously applied in the construction of the free energy curves.<sup>27</sup> To this end, energies related to reaction processes such as the free energies of reaction and activation are calculated and compared with those obtained from calculations with the PCM model<sup>16</sup> and AMBER force field.<sup>29</sup> The PCM model uses an ab initio energy to describe the solute and a continuum of dielectric constant  $\epsilon$  for the solvent. The AMBER potential uses quantum mechanically derived RESP charges<sup>30</sup> to calculate the electrostatic energy, and Lennard-Jones parameters derived from liquid properties<sup>31</sup> to calculate the van der Waals energy.

The hydration of ethene to give ethanol is a typical example of reactions of electrophilic and nucleophilic addition to the carbon–carbon double bond. This reaction, that usually takes place in an acid medium, in the absence of a catalyst can be regarded as an example of a proton addition process in an aqueous environment. The reaction can be schematized as the transfer of a water hydrogen (with the rupture of an O–H bond) to the carbon–carbon double bond to form a new bond (C–H), simultaneous with the rupture of the  $\pi$ -bond (C–C) and the formation of a covalent bond between the water oxygen and the other carbon atom (C–O).



Theoretical and experimental studies of this reaction have been carried out by several authors<sup>32–38</sup> providing structural and energy information that can be compared with that given by

\* Corresponding author. Telephone: +34-924289401. Fax: +34-924275576. E-mail: santi@unex.es.

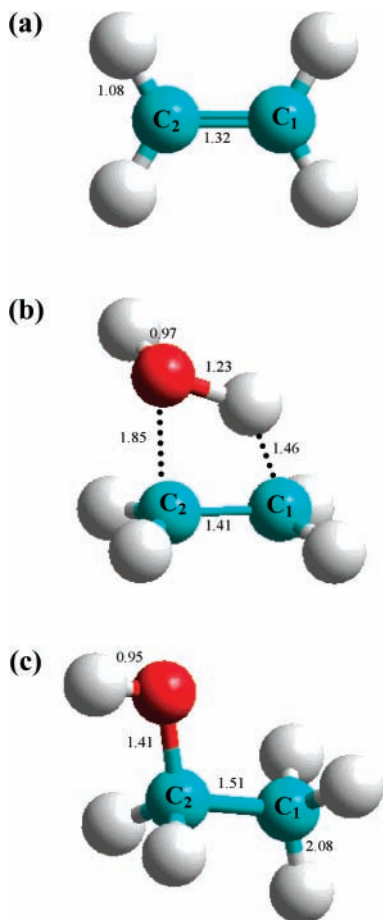
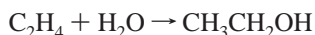


**Figure 1.** Geometry of the (a) reactant, (b) transition state, and (c) product molecules.

applying our model potential. We can thus validate the goodness of our proposed model for the theoretical study of chemical reactions in aqueous solution. Nevertheless it will be necessary to keep in mind, when comparing with other results, that our study deals with a concerted mechanism with the participation of one molecule of water, while most of the existing results come from stepwise mechanisms catalyzed by some acids.

## 2. Formalism and Calculation Details

**2.1. Geometry of the Molecules.** For this work, we chose the ethene and water molecules as reactants and the ethanol molecule as the product:



The geometries of the ethene, water, and ethanol involved in the simulations were determined at the MP2 level<sup>39</sup> with the “split-valence” 6-31G\* basis of Pople et al.<sup>40,41</sup> using the Gaussian/92 package,<sup>42</sup> and they are shown in Figure 1. The separation and relative orientation of the two solute molecules that form the transition state (ethene and water) were obtained in solution using the PCM model<sup>16</sup> at the MP2/6-31G\* level. Figure 1b shows the geometry of the transition state in which the hydrogen of the water molecule (whose bond is stretched up to 1.23 Å) is located near the carbon (at 1.46 Å) to favor the proton addition simultaneously with the nucleophilic attack of the OH<sup>-</sup> radical on the other carbon atom (separated by 1.85 Å). This transition state was verified by carrying out a normal-mode analysis, which provides a single imaginary frequency whose eigenvector corresponds to the simultaneous breaking

of the O–H and C–C bonds and forming of the C–O and C–H bonds, as well as deviation from planarity of the ethene fragment atoms. It is important to stress that the transition state corresponds to the simultaneous attack on the two carbon atoms of ethene, and that the mechanism of the reaction in solution can therefore be assumed to proceed through a single transition state, rather than stepwise.

**2.2. Potential Function and Parameters for the Solute–Solvent Interaction.** Several hundred values of the SCF and MP2 solute–solvent interaction energy were used to obtain the interaction parameters of the chosen potential energy function. In the present study, this was a Lennard-Jones 12-6 potential function that includes a Coulomb term in addition to the van der Waals terms:

$$U_{\text{sw}} = \sum_{ij} \frac{A_{ij}^{\text{sw}}}{r_{ij}^{12}} - \sum_{ij} \frac{B_{ij}^{\text{sw}}}{r_{ij}^6} + \sum_{ij} \frac{q_i^{\text{s}} q_j^{\text{w}}}{r_{ij}} \quad (1)$$

The net charges on each solute atom  $q_i^{\text{s}}$  were obtained using the ESIE procedure, which has been extensively described in previous work.<sup>19–28</sup> It can be summarized as fitting the values of the Coulomb electrostatic component of the interaction energy  $U_{\text{sw}}(\text{ES})$ , using the variational scheme of Morokuma and co-workers<sup>43, 44</sup> implemented in the GAMESS package<sup>45</sup> with the expression

$$U_{\text{sw}}(\text{ES}) = \sum_{ij} \frac{q_i^{\text{s}} q_j^{\text{w}}}{r_{ij}} \quad (2)$$

where the charges of the solvent water  $q_i^{\text{w}}$  are pre-assigned as the TIP3P charges.

The Lennard-Jones parameters  $A_{ij}^{\text{sw}}$  and  $B_{ij}^{\text{sw}}$  are obtained in a similar way to  $q_i^{\text{s}}$ , but now the energies used in the fits are those that describe the exchange (EX) and polarization (PL) components of the interaction energy at the SCF level and the dispersion (DIS) component related to the MP2 correlation energy:<sup>39</sup>

$$U_{\text{sw}}(\text{EX}) = \sum_{ij} \frac{A_{ij}^{\text{sw}}}{r_{ij}^{12}} \quad (3)$$

$$U_{\text{sw}}(\text{PL} + \text{DIS}) = \sum_{ij} \frac{B_{ij}^{\text{sw}}}{r_{ij}^6} \quad (4)$$

The parameters  $A_{ij}^{\text{sw}}$ ,  $B_{ij}^{\text{sw}}$ , and  $q_i^{\text{s}}$  are listed in Table 1 for the ethene, ethene–water, and ethanol systems. They were obtained either from the EX-PL-DIS-ES components or from the AMBER(ff99) force field, and they will henceforth be denoted as ABQ and AMBER parameters, respectively.

**2.3. Formalism for the Thermodynamic Study of Reaction Processes.** Knowledge of the energy curves that guide fluctuations of the solvent is particularly important in the study of chemical processes in solution because it allows one to calculate the reaction and activation energies of the process without the necessity of determining the reaction path. One of the most commonly used reaction coordinates is the difference in the solute–solvent interaction energy of a given set of solvent molecules in the presence of the reactant, transition state, and product structures,<sup>46</sup> for which one only needs the potential function that suitably describes this interaction. Thus, one can use the differences in the solute–water

**TABLE 1: Interaction Parameters<sup>a,b</sup> of Reactant, Transition State, and Product Molecules**

system	atom	ABQ			AMBER		
		$A_{ij}$	$B_{ij}$	$q_i$	$A_{ij}$	$B_{ij}$	$q_i$
ethene	C	515233.4	496.5	-0.462	696790.7	564.5	-0.332
	HC	9981.8	53.7	0.234	50543.6	98.2	0.166
ethanol	C <sub>1</sub>	2229758.8	1166.8	-0.475	785890.0	636.7	-0.126
	C <sub>2</sub>	228015.5	-139.3	0.578	785890.0	636.7	0.306
	O	405540.3	741.3	-0.365	582511.3	645.5	-0.682
	HC <sub>1</sub>	7383.7	42.4	0.149	69177.3	116.2	0.012
	HC <sub>2</sub>	117572.5	120.4	-0.346	69177.3	116.2	-0.018
	HO	3731.8	76.8	0.544	0.0	0.0	0.414
ethene-water	C <sub>2</sub>	704982.5	238.1	0.267	696790.7	564.5	0.281
	C <sub>1</sub>	1110286.2	596.6	-0.931	785890.0	636.7	-0.754
	O <sub>7</sub>	1228049.8	238.6	-0.980	582511.3	645.5	-0.743
	H <sub>3</sub> C <sub>2</sub>	20625.6	72.0	0.113	50543.6	98.2	-0.066
	H <sub>4</sub> C <sub>2</sub>	21298.6	30.8	0.164	50543.6	98.2	0.098
	H <sub>5</sub> C <sub>1</sub>	30276.8	98.4	0.240	69177.3	116.2	0.162
	H <sub>6</sub> C <sub>1</sub>	28526.7	14.8	0.256	69177.3	116.2	0.187
	H <sub>8</sub> O	2005.3	95.4	0.523	0.0	0.0	0.396
	H <sub>9</sub> C <sub>1</sub>	117253.3	99.4	0.363	0.0	0.0	0.304

<sup>a</sup> The van der Waals parameters (with the oxygen as the only interaction center) and charges in the solvent water are the TIP3P values. <sup>b</sup>  $A_{ij}$  in kcal Å<sup>12</sup> and  $B_{ij}$  in kcal Å.<sup>6</sup>

interaction energies ( $U_{sw}$ ) between the diabatic states of the solute in its product (P), transition state (TS), and reactant (R) structures for a broad set of configurations of solvent molecules around the solute in a simulation (S).

$$\Delta E_S = U_{SW,P} - U_{SW,R} \quad (5)$$

Thus, in the MD simulation of the reactant ( $S = R$ ), we divide the trajectory into  $N$  equally separated steps. At each of these steps, the interaction energies of the solvent with the solute in its reactant and product forms are calculated simultaneously ( $U_{SW,R}$  and  $U_{SW,P}$ ). In the same way, the interaction energies are calculated for the product simulation ( $S = P$ ) and transition state ( $S = TS$ ). In all cases, the difference  $\Delta E_S$  fluctuates, and its values are collected as a histogram of the number of times  $N_s$  that a particular value  $\Delta e$  of the macroscopic variable  $\Delta E_S$  appears in the simulation.

The probability  $P_s(\Delta e)$  of finding the system in a given configuration can be expressed

$$P_s(\Delta e) = \frac{\sum_{i=1}^{N_s} \delta(\Delta E_S(t_i) - \Delta e)}{N_s} \quad (6)$$

where  $\Delta E_S(t_i)$  is the value of the energy gap at the  $i$ th time step of the trajectory  $s$ . The delta function  $\delta$  is assigned a value 1 when  $|\Delta E_S(t_i) - \Delta e| \leq (\Delta e_{\max} - \Delta e_{\min})/2n_{\text{bins}}$ , and a value 0 otherwise, where  $\Delta e_{\max}$  and  $\Delta e_{\min}$  are the maximum and minimum values of the  $\Delta e$  that occurs during the trajectory and  $n_{\text{bins}}$  is the number of bins used to construct the histogram.<sup>46-48</sup>

The free energy  $G_S(\Delta e)$  is computed from the normalized probability distribution of the variable  $\Delta e$ :

$$G_S(\Delta e) = -k_B T \ln P_s(\Delta e) \quad (7)$$

Next, a search is made for the polynomial function that best fits these free energies, and the result is plotted. To obtain analytically the value of the reaction and activation energies, the curve  $G_P$  is made to coincide at the point of minimum energy

of the curve  $G_R$ , where the separation between the two minima is

$$\Delta G(x_p = \Delta e_{\text{eq}}^R; x_p = \Delta e_{\text{eq}}^P) = G_{\text{eq}}^P - G_{\text{eq}}^R = a(\Delta e_{\text{eq}}^R - \Delta e_{\text{eq}}^P) + b(\Delta e_{\text{eq}}^R - \Delta e_{\text{eq}}^P)^2 + c(\Delta e_{\text{eq}}^R - \Delta e_{\text{eq}}^P)^3 + \dots \quad (8)$$

with  $\Delta e_{\text{eq}}^P$  and  $\Delta e_{\text{eq}}^R$  being the most probable values of  $\Delta E$  in the free energy curves  $G_P$  and  $G_R$ , respectively, and  $a$ ,  $b$ , and  $c$  are the coefficients of the polynomial fit to the curve  $G_P$ .

**2.4. Simulation Details.** Molecular dynamics simulations of an NVT ensemble of a solute molecule in an aqueous environment formed by 210 water molecules were carried out at 298 K using the AMBER program.<sup>29</sup> The time considered for the simulations was 1200 ps with time steps of 0.1 fs. The first 200 ps were taken to ensure that the equilibrium is reached completely, and the last 1000 ps were stored to configurations of the water molecules required for the determination of the thermodynamic and structural properties studied in this work. The water molecules initially located at distances less than 1.6 Å from any solute atom were eliminated from the simulations.

The long-range electrostatic interactions were treated by the Ewald method,<sup>49</sup> and the solutes were kept rigid using the shake algorithm.<sup>50</sup> A cutoff of 5 Å was applied to the water-water interactions to simplify the calculations, and periodic boundary conditions were used to keep the number of solvent molecules constant. The solute-solvent interactions were calculated with the potential function LJ(12-6-1), using the parameters obtained from fitting the EX-PL-DIS-ES components or those from the AMBER(ff99) field forces, while for the solvent-solvent interactions the potential TIP3P of Jorgensen<sup>51</sup> was employed.

Finally, in calculating the differences  $\Delta E_S$  and building the  $\Delta G_S$  free energy curves it is necessary to keep in mind that in the configurations stored during the simulation of one of the molecules, the other molecule must be displaced to the position occupied by the first and reoriented in order to reproduce the distribution of their atoms.

## Results and Discussion

Inspection of Table 1 shows that our ABQ potential leads to systems with greater charges than those obtained with the AMBER potential in all the molecules considered (reactant, transition state, and product). It is necessary to emphasize that

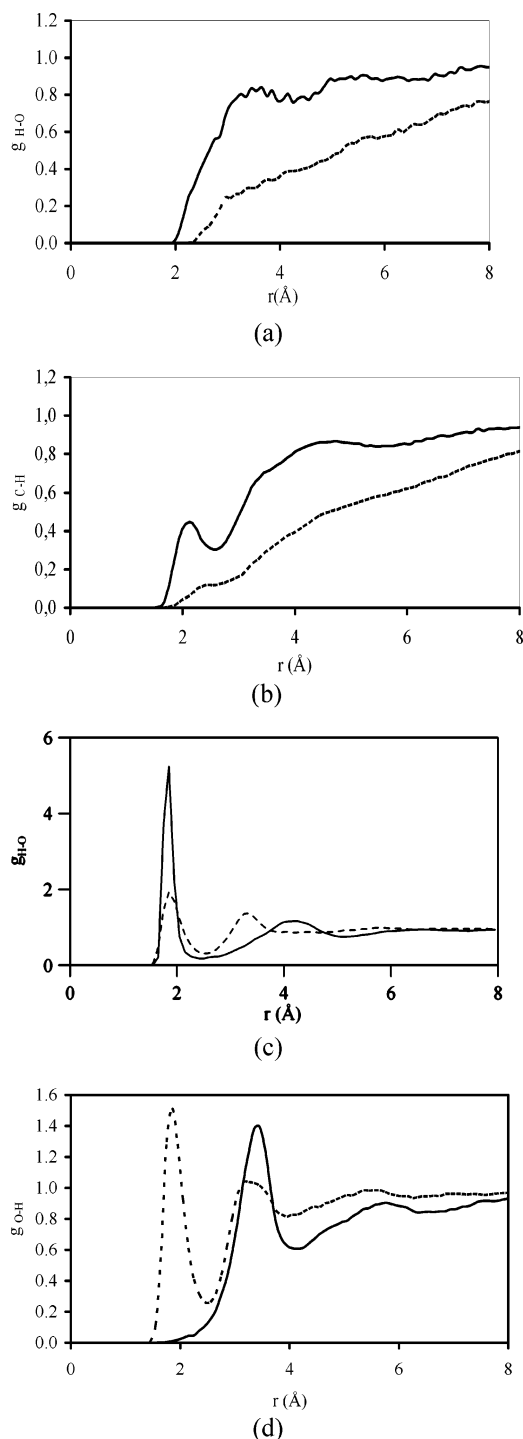


**Figure 2.** Radial distribution functions with ABQ (---) and AMBER (—) potentials: (a)  $g_{\text{H-O}}$ , and (b)  $g_{\text{C-H}}$  for ethene; (c)  $g_{\text{H-O}}$  and (d)  $g_{\text{O-H}}$  for ethanol.

the RESP and ESIE charges describe the O–H bond of the ethanol molecule differently. Thus, with our potential, the hydroxyl hydrogen is more charged while part of the charge of the oxygen is transferred to the hydrogens of the group  $-\text{CH}_2$ . Furthermore, the terminal group  $\text{CH}_3$  appears more charged with our parameters.

This result leads to a greater hydration of the solute, and it is in consonance with the radial distribution functions shown in Figure 2. The shape of the  $g_{\text{sw}}$  functions (where  $s$  represents any solute atom and  $w$  any atom of the water solvent) in the ethene molecule show some degree of similarity with both potentials, although the ESIE curve is always higher, justifying

**TABLE 2: Solute–Solvent Interaction Energies and Free Energies Associated with the Reaction Process<sup>a</sup>**

	AMBER	ABQ	HF-PCM <sup>e</sup>	MP2(Full)/6311G(d,p) <sup>f</sup>
$\langle \Delta U_{\text{sw}} \rangle^b$	1.51	−6.84		
$\langle \Delta U_{\text{sw}}^\# \rangle^c$	16.81	16.67		
$\Delta G^b$	−3.70	−14.6 (−14.7) <sup>d</sup>	−16.18	−9.4
$\Delta G^\#^c$	0.45	36.27 (14.7) <sup>d</sup>	91.26	67.1

<sup>a</sup> In kcal/mol. <sup>b</sup> Reaction energy for ethene + water  $\rightarrow$  ethanol process. <sup>c</sup> Activation energy for ethanol  $\rightarrow$  ethene + water process. <sup>d</sup> Results in parenthesis are obtained using only the R and P free energy curves. <sup>e</sup> Values obtained using the polarizable continuum model and HF energies. <sup>f</sup> Refs 33, 34.

the greater hydration (notice that in the ESIE case the bond of the solvent with the solute carbon atom is favored, with a first peak at 2 Å and a second more intense peak at 4 Å). For the ethanol solute, something similar is the case, although we have to stress that some functions have their peaks shifted with respect to the result obtained with the RESP charges. Thus, for example, the function  $g_{\text{O-H}}$  with our potential has a first maximum at approximately 3 Å, outside the typical region of the hydrogen bond, while for the  $g_{\text{H-O}}$  function the first peak is much more intense with our ESIE charges. These results can be explained by the different charge on the hydroxylic bond atoms in the alcohol, since when we move from the AMBER to the ESIE parameters, the charge on the oxygen atom is reduced in half, and therefore the aqueous solvent is more weakly attracted and the distance between solute and solvent increases. Conversely, the charge on the hydrogen atom increases by 0.1  $e^-$ , leading to an increase in the intensity of the peak observed in the  $g_{\text{H-O}}$  function.

Comparing the water molecules in the first solvation shell of the ethanol molecule obtained from integration of the  $g_{\text{O-O}}$  and  $g_{\text{C-O}}$  functions up to the first minimum, one can say that the values of 3 and 16 obtained with the two charge models are close to the 3.3<sup>52</sup> and 18<sup>53</sup> experimental values. Also, in the ethene molecule the coordination number of the carbon atom obtained at 6 Å with our potential is 19 molecules, in good agreement with the result of 23 water molecules given by van Erp and Meijer.<sup>35</sup>

In the solvation process, the ethanol molecule presents an average solute–solvent interaction energy of  $-24.87$  kcal/mol, larger than the  $-5.01$  and  $-13.02$  kcal/mol values for the ethane and water reactants respectively, with a reaction exothermicity of  $\langle \Delta U_{\text{sw}} \rangle = -6.84$  kcal/mol computed with our parameters. Intermediate between these values is the  $-8.20$  kcal/mol of the interaction of the transition state with the aqueous solvent and, therefore, an activation energy of  $\langle \Delta U_{\text{sw}}^\# \rangle = 16.67$  kcal/mol with our method. It is also important to mention that the ABQ potential model gives a greater interaction energy in all the molecules as a consequence of the more charged solute (compare the aforementioned ABQ potential values with the  $-1.90$ ,  $-13.41$ , and  $+3.40$  kcal/mol for ethane, ethanol, and transition state using the AMBER parameters). With all these values, we perform an estimation of the reaction and activation energies (see Table 2), finding that with our parameters the reaction is more exothermic, while the activation barrier is by chance similar with the two potentials. One can say that the reaction of formation of ethanol from ethene in solution is accompanied initially by a decrease (R $\rightarrow$ TS process) and then by an increase (TS $\rightarrow$ P process) in the molecular hydration. Nevertheless these reaction and activation energies, obtained taking into account only the solute–solvent interaction energies  $U_{\text{sw}}$ , are far from the available values, therefore making it necessary to perform

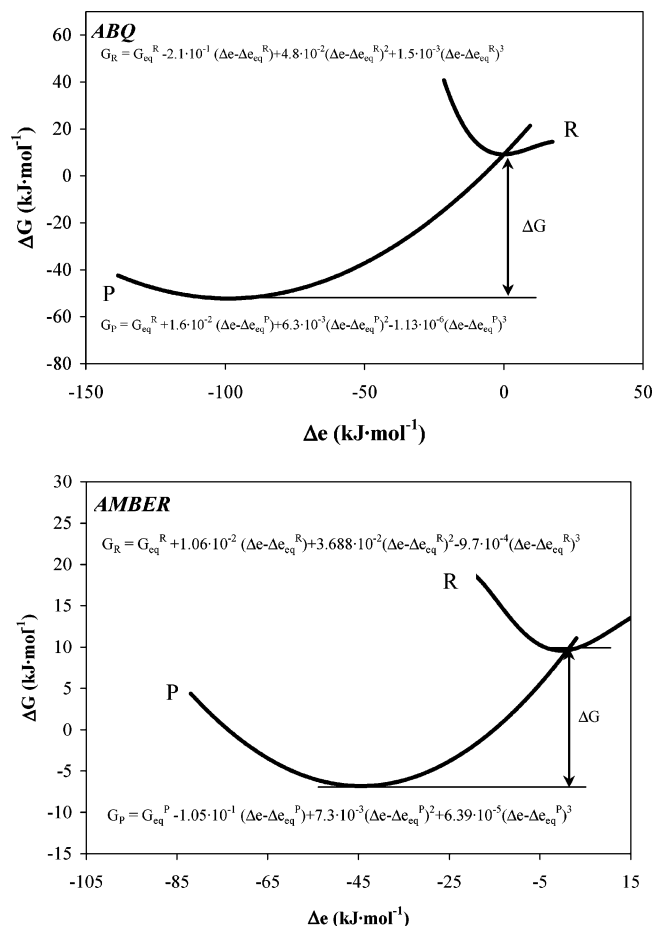


**Figure 3.** Free energy curves for R and P simulations with ABQ and AMBER potentials.

a more appropriate analysis where other energies such as the solvent relaxation or entropy contributions are considered.

To calculate the reaction and activation free energies, we constructed the R, TS, and P diabatic free energy curves shown in Figures 3 and 4, following a procedure similar to that employed by Ando and Hynes for acid ionization in water.<sup>54,55</sup> The relative positions of these curves were corrected in accordance with the work of Tachiya,<sup>56</sup> so that the curves are vertically shifted at the point where  $\Delta e^P = \Delta e_{eq}^{R(TS)}$ , making it possible to apply eq 8. With both potentials, the curves corresponding to the product are somewhat deeper than those of the reactant and transition state, leading to exothermic reactions with noticeable barrier energies.

Given that the computed free energy of this reaction is  $-9.4$  kcal/mol with an MP2 treatment,<sup>33,34</sup> and  $-9.09$  kcal/mol with a BLYP-CPMD model,<sup>35-37</sup> one can conclude that the results obtained with our electrostatic and van der Waals parameters describe reasonably well the reaction energy, and significantly better than when the AMBER parameters are used in the LJ(12-6-1) potential function and when the effect of the solvent as a dielectric is considered (see values  $\Delta G$  in Table 2).

Comparing the values of the activation free energy in the ethanol formation with those from experimental studies, one observes an appreciable difference between the two potentials used. Of particular interest in these experimental studies is the work of Baliga and Whalley,<sup>32</sup> in which they measured the hydration of ethene in dilute aqueous perchloric acid in the range of  $170-190$  °C at 100 bar, and estimated a barrier height of  $33.3 \pm 1.0$  kcal/mol. This value would be higher when the catalyst is absent. For example, MP2(FULL)/6-311G(d,p)

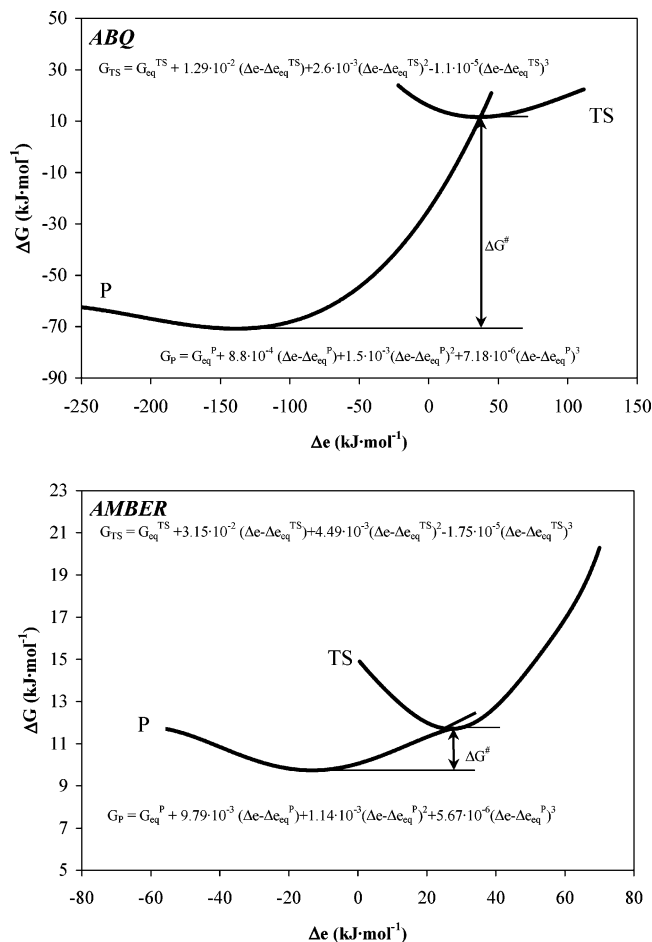


**Figure 4.** Free energy curves for TS and P simulations with ABQ and AMBER potentials.

calculations give barriers of  $67.1$  kcal/mol,<sup>33,34</sup> and BLYP/6-31G\* calculations give  $64.4$  kcal/mol<sup>38</sup> for the reaction of ethanol dehydration. The present values of the free energy activation are very far from any of the theoretical values (the ab initio results suggest that the threshold energy for the elimination water from ethanol is  $\leq 76$  kcal/mol), although our potential improves the results of this energy noticeably compared to those obtained using the AMBER parameters. In this regard, it is interesting to note that the activation energy was notably improved when  $\Delta G$  was fitted to polynomial functions and when the free energy curve associated with the transition state was taken into account in the calculation, since applying the traditional fit to quadratic functions and considering only the R and P free energy curves yields results of  $14.7$  kcal/mol (see values in parentheses of Table 2).

## Conclusions

In summary, the use of simple potentials of the type LJ(12-6-1) to describe the solute-solvent interactions in the molecular dynamics simulation of chemical reactions in an aqueous medium, and to obtain free energy curves, leads to acceptable results when the interaction parameters are chosen appropriately. Thus, when one uses the ESIE charges and the  $A_{ij}^{sw}$  and  $B_{ij}^{sw}$  parameters determined from the EX-PL-DIS components of the interaction energy, the results for the free energy of reaction are in acceptable agreement with the available theoretical and experimental data. Nevertheless, although the activation energy obtained with our potential model is better than that resulting from using AMBER parameters, it seems necessary to consider

a better description of the solute–solvent interaction parameters (improving the description of the electrostatic, exchange repulsion, polarization, and dispersion contributions to the interaction energies) and of the transition state structure (considering that several water molecules can take part in the transition state through a stepwise mechanism) to obtain acceptable values of this property. These considerations are, however, beyond the objectives pursued in this work, focused in showing that the used methodology is applicable to the study of reactions in aqueous solution.

**Acknowledgment.** This research was sponsored by the Consejería de Infraestructuras y Desarrollo Tecnológico de la Junta de Extremadura (Project GRU07013).

## References and Notes

- (1) Cramer, C. J.; Truhlar, D. G. *Structure and Reactivity in Aqueous Solution*; American Chemical Society: Washington, DC, 1994.
- (2) Warshel, A. *Computer Modeling of Chemical Reactions in Enzymes and Solutions*; Wiley & Sons: New York, 1991.
- (3) Jorther, J.; Levine, R. D.; Pullman, B. *Reaction Dynamics in Cluster and Condensed Phases*; Kluwer Academic Publishers: London, 1999.
- (4) Moreau, M.; Turq, P. *Chemical Reactivity in Liquids. Fundamental Aspects*; Plenum: New York, 1988.
- (5) Honeisel, C. *Theoretical Treatment of Liquids and Liquid Mixtures*; Elsevier: New York, 1993.
- (6) Politzer, P.; Murray, J. S. *Quantitative Treatments of Solute-Solvent Interactions*; Elsevier: Amsterdam, 1994.
- (7) Simkin, B. Y.; Shekhet, I. I. *Quantum Chemical and Statistical Theory of Solutions. A Computational Approach*; Ellis Horwood: Madrid, 1995.
- (8) Truhlar, D. G.; Isaacson, A. D.; Garret, B. C. *The Theory of Chemical Reaction Dynamics*, Vol. 4; Baer, M., Ed.; CRC Press: Boca Raton, FL, 1985.
- (9) Muller, A.; Ratczak, H.; Junge, W.; Diemann, E. *Electron and Proton Transfer in Chemistry and Biology*; Elsevier: New York, 1992.
- (10) Bala, P.; Grocowski, P.; Lesyg, B.; McCammon, J. A. *Quantum Mechanical Simulation Methods for Studying Biological Systems*; Bicout, D., Field, M., Eds.; Springer: Berlin, 1995.
- (11) Gao, J. *Methods and Applications of Combined Quantum Mechanical and Molecular Mechanical Potentials. VCH Reviews in Computational Chemistry*, Vol. 7; Lipkowitz, K. B., Boyd, B. D., Eds.; VCH Publishers: New York, 1996.
- (12) Rivail, J. L. *New Theoretical Concepts for Understanding Organic Reactions*; Bertrán, J., Csizmadia, I. G., Eds.; Kluwer: Dordrecht, 1989.
- (13) Cramer, C. J.; Truhlar, D. G. *Solvent Effects and Chemical Reactivity*; Tapia, O., Bertran, J., Eds.; Kluwer: Dordrecht, 1996.
- (14) Hynes, J. T. *Solvent Effects and Chemical Reactivity*; Tapia, O., Bertran, J., Eds.; Kluwer: Dordrecht, 1996.
- (15) Truhlar, D. G. *The Reaction Path in Chemistry: Current Approaches and Perspectives*; Heidrich, D., Ed.; Kluwer: Dordrecht, 1995.
- (16) Miertus, S.; Scrocco, E.; Tomasi, J. *J. Chem. Phys.* **1981**, *55*, 117.
- (17) Gao, J. *J. Chem. Phys.* **1992**, *96*, 537.
- (18) Alder, B. J.; Winwright, T. E. *J. Chem. Phys.* **1959**, *31*, 459.
- (19) Tolosa, S.; Sansón, J. A.; Hidalgo, A. *Chem. Phys.* **2001**, *265*, 207.
- (20) Tolosa, S.; Sansón, J. A.; Hidalgo, A. *Chem. Phys. Lett.* **2002**, *357*, 279.
- (21) Tolosa, S.; Sansón, J. A.; Hidalgo, A. *Recent Research Developments in Chemical Physics*; Transworld Research Network, 2002.
- (22) Tolosa, S.; Sansón, J. A.; Hidalgo, A. *Chem. Phys.* **2003**, *293*, 193.
- (23) Tolosa, S.; Sansón, J. A.; Hidalgo, A. *J. Solution Chem.* **2005**, *34*, 407.
- (24) Tolosa, S.; Sansón, J. A.; Hidalgo, A. *Chem. Phys.* **2005**, *315*, 76.
- (25) Tolosa, S.; Sansón, J. A.; Hidalgo, A. *Mol. Simul.* **2005**, *31*, 549.
- (26) Tolosa, S.; Sansón, J. A.; Hidalgo, A. *Chem. Phys.* **2006**, *327*, 187.
- (27) Tolosa, S.; Sansón, J. A.; Hidalgo, A. *J. Phys. Chem. A* **2007**, *111*, 339.
- (28) Tolosa, S.; Sansón, J. A.; Hidalgo, A. *Quantum Chemistry Research Trends*; Kaisas, M. P., Ed.; Nova Science Publisher: New York, 2007.
- (29) Case, D. A.; Darden, T. A.; Cheatham, T. E., III; Simmerling, C. L.; Wang, J.; Duke, R. E.; Luo, R.; Mert, K. M.; Wang, B.; Pearlman, D. A.; Crowley, M.; Brozell, S.; Tsui, V.; Gohlke, H.; Mongan, J.; Hornak, V.; Cui, G.; Beroza, P.; Schafmeister, C.; Caldwell, J. W.; Ross, W. S.; Kollman, P. A. *AMBER 8*; University of: San Francisco, 2004.
- (30) Shirts, M. R.; Pitera, J. W.; Swope, W. C.; Pande, V. S. *J. Chem. Phys.* **2003**, *119*, 5740.
- (31) Jorgensen, W. L.; Tirado-Rives, J. *J. Am. Chem. Soc.* **1988**, *110*, 1657.
- (32) Baliga, B. T.; Whalley, E. *Can. J. Chem.* **1965**, *43*, 2453.
- (33) Butkovskaya, N. I.; Setser, D. W. *J. Phys. Chem.* **1994**, *98*, 10779.
- (34) Butkovskaya, N. I.; Setser, D. W. *J. Chem. Phys.* **1996**, *105*, 8064.
- (35) Van Erp, T. S.; Meijer, E. J. *J. Chem. Phys.*, **2003**, *118*, 8831.
- (36) Van Erp, T. S. Ph.D. Thesis, Universitet van Amsterdam, 2003.
- (37) Meijer, E. J. *Angew. Chem., Int. Ed.* **2004**, *43*, 1660.
- (38) Nakagama, Y.; Tjima, N.; Hirao, K. *J. Comput. Chem.* **2000**, *21*, 1292.
- (39) Moller, C.; Plesset, M. S. *Phys. Rev.* **1934**, *46*, 618.
- (40) Ditchfield, R.; Hehre, W. J.; Pople, J. A. *J. Chem. Phys.* **1971**, *54*, 724.
- (41) Hehre, W. J.; Ditchfield, R.; Pople, J. A. *J. Chem. Phys.* **1972**, *56*, 2257.
- (42) Frisch, M. J.; Trucks, G. W.; Head-Gordon, M.; Gill, P. M. W.; Wong, M. W.; Johnson, B. G.; Schlegel, H. B.; Robb, M. A.; Replogle, E. S.; Gomperts, R.; Andres, J. L.; Raghavachari, K.; Binkley, J. S.; Gonzalez, C.; Martín, R. L.; Fox, D. J.; DeFrees, D. J.; Baker, J.; Stewart, J. J. P.; Pople, J. A. *GAUSSIAN/92*, Revision D.3; Gaussian Inc.: Pittsburgh, 1992.
- (43) Morokuma, K. *J. Chem. Phys.* **1970**, *19*, 553.
- (44) Kitaura, K.; Morokuma, K. *Int. J. Quantum Chem.* **1976**, *10*, 325.
- (45) Dupuis, M.; Spangler, D.; Wendoloski, J. *GAMESS Program QG01*; National Resource for Computations in Chemistry Software Catalog; University of California: Berkeley, CA, 1980.
- (46) Carter, E. A.; Hynes, J. T. *J. Phys. Chem.* **1989**, *93*, 2184.
- (47) King, G.; Warshel, A. *J. Chem. Phys.* **1990**, *93*, 8682.
- (48) Kuharski, R. A.; Bader, J. S.; Chandler, D.; Sprik, M.; Klein, M. L.; Impey, R. W. *J. Chem. Phys.* **1988**, *89*, 3248.
- (49) Ewald, P. *Ann. Phys.* **1921**, *64*, 253.
- (50) Ryckaert, P.; Ciccotti, G.; Berendsen, J. J. C. *J. Comput. Phys.* **1977**, *23*, 237.
- (51) Mahoney, M. W.; Jorgensen, W. L. *J. Chem. Phys.* **2000**, *20*, 8910.
- (52) Sidhu, S. K.; Godfellow, M. J.; Turner, Z. J. *J. Chem. Phys.* **1999**, *110*, 793.
- (53) Petrillo, C.; Onori, G.; Sacchetti, F. *Mol. Phys.* **1989**, *67*, 697.
- (54) Ando, K.; Hynes, J. T. *J. Phys. Chem. B* **1997**, *101*, 10464.
- (55) Ando, K.; Hynes, J. T. *J. Phys. Chem. A* **1999**, *103*, 10398.
- (56) Tachiya, M. *J. Chem. Phys.* **1989**, *93*, 7050.